

CrossMark  
click for updatesCite this: *Chem. Sci.*, 2017, 8, 600Received 3rd August 2016  
Accepted 30th August 2016

DOI: 10.1039/c6sc03450k

www.rsc.org/chemicalscience

# Carbon dioxide binding at a Ni/Fe center: synthesis and characterization of Ni( $\eta^1$ -CO<sub>2</sub>- $\kappa$ C) and Ni- $\mu$ -CO<sub>2</sub>- $\kappa$ C: $\kappa^2$ O,O'-Fe<sup>†</sup>

Changho Yoo and Yunho Lee\*

The degree of CO<sub>2</sub> activation can be tuned by incorporating a distinct electronic coordination environment at the nickel center. A mononuclear nickel carboxylate species (Ni-CO<sub>2</sub>, **3**) and a dinuclear nickel-iron carboxylate species (Ni-CO<sub>2</sub>-Fe, **5**) were prepared. The structure of **3** reveals a rare  $\eta^1$ - $\kappa$ C binding mode of CO<sub>2</sub>, while that of **5** shows bridging CO<sub>2</sub> binding ( $\mu_2$ - $\kappa$ C: $\kappa^2$ O,O') between the nickel and iron, presented as the first example of a nickel- $\mu$ -CO<sub>2</sub>-iron species. The structural analyses of **3** and **5** based on XRD and DFT data reveal a higher degree of CO<sub>2</sub> activation in **5**, imparted by the additional interaction with an iron ion.

## Introduction

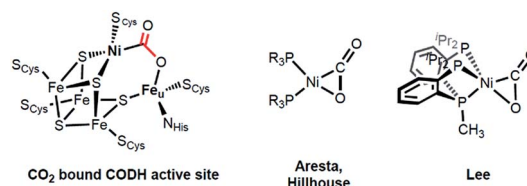
Activation of carbon dioxide is currently receiving much attention due to its relevance to environmental and energy related issues.<sup>1</sup> In the area of transition metal catalyzed reactions, one of the main challenges is selective reduction of CO<sub>2</sub> to a product such as formate, carbon monoxide, methanol or methane.<sup>2</sup> In a 2-electron process, the binding mode of the CO<sub>2</sub> may determine the eventual product formation, *e.g.* formate *vs.* carbon monoxide.<sup>3</sup> When the initial metal-oxygen interaction occurs to form a metal CO<sub>2</sub> adduct M- $\eta^1$ -CO<sub>2</sub>- $\kappa$ O, subsequent hydride transfer *via* CO<sub>2</sub> addition to a M-H bond generates a metal-formate species. Alternatively, the metal-carbon bond formation can produce a metallocarboxylate species (M- $\eta^1$ -CO<sub>2</sub>- $\kappa$ C), followed by C-O bond cleavage to generate CO. In the latter case, an additional Lewis acid interaction can stabilize the negative charges at the oxygen atoms of the bound CO<sub>2</sub>.<sup>4,5</sup> Therefore, CO<sub>2</sub> activation with a bimetallic system can be one way to guide the selectivity of the CO<sub>2</sub> catalyst and is receiving much attention.<sup>5,6</sup> In fact, an excellent example of a bimetallic center utilized in an efficient catalytic conversion of CO<sub>2</sub> can be found in the active site of carbon monoxide dehydrogenase (CODH).<sup>7</sup> According to recent studies, CO<sub>2</sub> coordination at a heterobimetallic nickel-iron active site can be found in CODH's intermediate species, which possesses a Ni- $\mu$ -CO<sub>2</sub>-Fe moiety, Scheme 1.<sup>8</sup> Although X-ray analysis provides a structural snapshot of the CO<sub>2</sub> reduction sequence, the role of the unique

iron ion is currently not well-understood.<sup>7</sup> Thus, acquiring an understanding of iron assisted CO<sub>2</sub>-nickel coordination is of fundamental interest and is crucial for gaining mechanistic insight into this and other enzymatic reactions.

In organonickel chemistry, there are few mononuclear Ni- $\eta^2$ -CO<sub>2</sub> adducts possessing both M-C and M-O bonds.<sup>9</sup> In 1975, Aresta and co-workers reported the first structurally characterized nickel-CO<sub>2</sub> adduct (PCy<sub>3</sub>)<sub>2</sub>Ni( $\eta^2$ -CO<sub>2</sub>), Scheme 1.<sup>9a</sup> An analogous complex, (dtbpe)Ni( $\eta^2$ -CO<sub>2</sub>) (dtbpe = 1,2-bis(di-*tert*-butylphosphino)ethane) was recently reported by Hillhouse and co-workers.<sup>9d</sup> More recently, our group reported a similar but unique five-coordinate nickel-CO<sub>2</sub> adduct (PP<sup>Me</sup>P)Ni( $\eta^2$ -CO<sub>2</sub>) (PP<sup>Me</sup>P = PMe(2-P<sup>i</sup>Pr<sub>2</sub>-C<sub>6</sub>H<sub>4</sub>)<sub>2</sub>).<sup>9f</sup> According to its structural analysis, the five coordinate nickel CO<sub>2</sub> species supported by three neutral P donors has a weak Ni-O bond available for electrophilic attack.<sup>9f</sup> Additionally, by utilizing an anionic tridentate PNP ligand (PNP<sup>-</sup> = N[2-P<sup>i</sup>Pr<sub>2</sub>-4-Me-C<sub>6</sub>H<sub>3</sub>]<sub>2</sub><sup>-</sup>), our group reported the nickel hydroxycarbonyl species (PNP)NiCOOH (**1**), (PNP)NiCOONa (**2**) and {(PNP)Ni}<sub>2</sub>- $\mu$ -CO<sub>2</sub>- $\kappa^2$ C,O (**4**), the first examples of Ni-CO<sub>2</sub> complexes that reveal a Ni-CO<sub>2</sub>- $\kappa$ C binding mode, Scheme 2.<sup>10</sup> The carboxylate group in these species is stabilized by a Lewis acid such as a proton, sodium or another nickel ion. Our interest then moved to comparing (PP<sup>Me</sup>P)Ni-

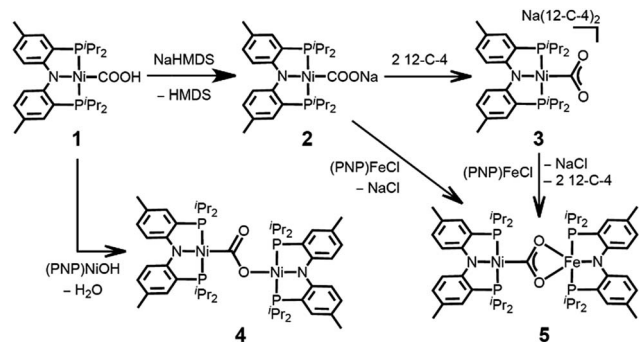
Department of Chemistry, Korea Advanced Institute of Science and Technology (KAIST), Daejeon 34141, Republic of Korea. E-mail: yunholee@kaist.ac.kr; Fax: +82 42 350 2810; Tel: +82 42 350 2814

<sup>†</sup> Electronic supplementary information (ESI) available: Characterization data for **3** and **5**. CCDC 1492006 and 1492007. For ESI and crystallographic data in CIF or other electronic format see DOI: 10.1039/c6sc03450k



Scheme 1 The active site of carbon monoxide dehydrogenase (CODH, left), and 4- and 5-coordinate nickel CO<sub>2</sub> adducts (right).



Scheme 2 Preparation of mononuclear- and dinuclear-CO<sub>2</sub> adducts.

CO<sub>2</sub> and (PNP)Ni-CO<sub>2</sub> to evaluate their fundamental differences in CO<sub>2</sub> activation. The different geometries favored with a PP<sup>Me</sup>P or PNP ligand affect the identity of the nickel-CO<sub>2</sub> moiety, which can be Ni(II)-CO<sub>2</sub><sup>2-</sup> or Ni(0)-CO<sub>2</sub> or an open-shell Ni(I)-CO<sub>2</sub><sup>-</sup>, *vide infra*. Furthermore, by isolating the native nickel-CO<sub>2</sub> species, we can further study the effect of the second iron ion. Although several nickel carboxylate species are already known, iron has never been introduced synthetically into a Ni-CO<sub>2</sub> moiety.

Here, we present a nickel carboxylate species {Na(12-C-4)}<sub>2</sub>{(PNP)Ni-η<sup>1</sup>-CO<sub>2</sub>-κC} (3), in which the nickel-CO<sub>2</sub> moiety does not have any Lewis acid interactions. We also prepared a dinuclear nickel-iron carboxylate species (PNP)Ni-μ-CO<sub>2</sub>-κC:κ<sup>2</sup>O,O'-Fe(PNP) (5), reminiscent of the NiFe-binuclear active site of CODH. This is an unprecedented example of a nickel-iron hetero-bimetallic complex possessing a bridging CO<sub>2</sub> ligand. The levels of CO<sub>2</sub> activation in compounds 3 and 5 are compared with other Ni-CO<sub>2</sub> adducts and the Ni-μ-CO<sub>2</sub>-Fe moiety found in CODH.

## Results and discussion

### Synthesis and characterization of the Ni-η<sup>1</sup>-CO<sub>2</sub>-κC complex

The coordination of a hydroxycarbonyl moiety *via* a Ni-C bond was previously realized at a divalent nickel center supported by a PNP ligand.<sup>10</sup> Following deprotonation of (PNP)NiCOOH (1), its anionic congener (PNP)NiCOONa (2) was also prepared and recently reported by our group.<sup>10</sup> The X-ray structure reveals that two molecules of 2 are oriented to form a pair with ionic interactions with two sodium ions in the crystal lattice, Fig. 1.<sup>11</sup> The corresponding CO<sub>2</sub> ligand coordinates to the nickel center in a μ<sub>3</sub>-κ<sup>1</sup>C:κ<sup>2</sup>O,O':κ<sup>1</sup>O' mode with a Ni-C1 bond distance of 1.882(1) Å. There are additional bonds of the CO<sub>2</sub> moiety to sodium ions with Na-O bond distances of 2.352(1), 2.217(1) and 2.459(1).<sup>11</sup> To obtain a sodium-free adduct, 2 equiv. of 12-crown-4 was added to a solution of 2, resulting in the formation of {Na(12-C-4)}<sub>2</sub>{(PNP)Ni-η<sup>1</sup>-CO<sub>2</sub>-κC} (3). The crystal structure of 3 revealed the successful generation of a mononuclear nickel adduct possessing an η<sup>1</sup>-κC coordinated carbon dioxide species with a Ni-C bond distance of 1.911(2) Å, as shown in Fig. 1 and Table 1. The oxidation state of the nickel ion in 3 can be assigned as 2+ based on its similar structural features to

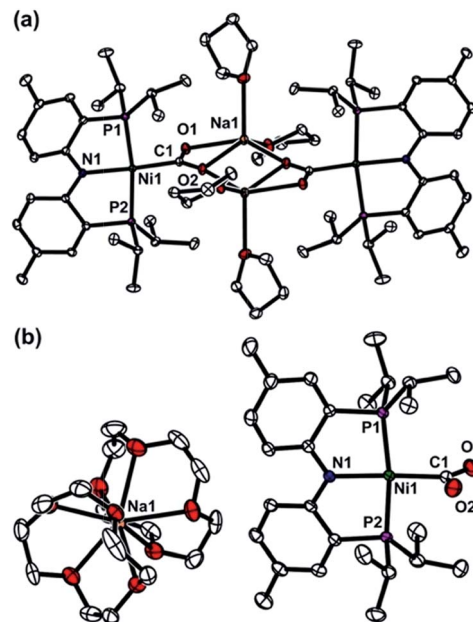


Fig. 1 Displacement ellipsoid (50%) representations for (a) (PNP)NiCOONa (2) in a dimeric assembly with co-crystallized THF molecules,<sup>11</sup> and (b) {Na(12-C-4)}<sub>2</sub>{(PNP)Ni-η<sup>1</sup>-CO<sub>2</sub>-κC} (3). A co-crystallized 12-crown-4 molecule and hydrogen atoms are omitted for clarity.

previously known nickel(II) species such as (PNP)NiCOOH (1) and {(PNP)Ni}<sub>2</sub>-μ-CO<sub>2</sub>-κ<sup>2</sup>C,O (4), *vide infra*. The geometry of 3 is square planar ( $\tau_4 = 0.12^{12}$ ) with a similar but slightly elongated Ni-C bond distance in comparison to those of 1 and 4 ( $d_{\text{Ni-C}} = 1.866(2)$  and 1.888(2) Å, respectively, Table 1). This is probably due to a lower degree of  $\pi$  back-bonding between the nickel and CO<sub>2</sub>. In fact,  $\pi$  back-donation from the nickel center to a CO<sub>2</sub> ligand in such nickel carboxylate species is indicated by shorter Ni-C distances (1.858–1.911 Å) than those of the nickel alkyl species (PNP)NiR (R = Me, Et, <sup>n</sup>Pr) (1.963–2.004 Å).<sup>13</sup> The molecular orbitals generated from DFT calculations also show the presence of  $\pi$  back-donation from the Ni  $d_{xz}$  to the CO<sub>2</sub>  $\pi^*$  orbital (see ESI†). Due to the absence of Lewis acid interactions in 3, a lower  $\pi$ -accepting ability of the CO<sub>2</sub> ligand is expected. Its structural data also revealed that the plane of the CO<sub>2</sub> ligand is perpendicular to that of the square planar (PNP)Ni moiety. One of the oxygen atoms ( $d_{\text{Ni-O}_2} = 2.614(1)$  Å) is slightly closer to the nickel center than the other ( $d_{\text{Ni-O}_1} = 2.776(1)$  Å), Table 2. These Ni-O distances are much longer than those for other known Ni-η<sup>2</sup>-CO<sub>2</sub> adducts (1.9–2.2 Å, Table 2), suggesting that neither of the oxygen atoms are bound.<sup>9</sup> The DFT analysis also supports minimal interaction between the nickel and oxygen atoms (Wiberg index = 0.1358 for Ni1-O2 and 0.1679 for Ni1-O1, see Table 2). The two C-O bond distances are nearly identical ( $d_{\text{C1-O}_1} = 1.247(2)$  Å,  $d_{\text{C1-O}_2} = 1.248(2)$  Å, Table 1) and slightly shorter than in the analogous carboxylate complexes 2 and 4 (Table 1), due to the absence of a Lewis acid, Na or Ni. According to the DFT analysis, the HOMO of 3 possesses contributions from both a nickel  $d_{x^2-y^2}$  orbital and a CO<sub>2</sub>  $\pi^*$  orbital, see Fig. 2. Due to additional electron density from



Table 1 Selected bond distances and angles for the nickel carboxylate species 1, 2, 3, 4 and 5, and CO<sub>2</sub>-bound CODH<sup>8b</sup>

	1 <sup>10</sup>	2 <sup>11</sup>	3	4 <sup>10</sup>	5	CODH <sup>8b</sup>
$d_{\text{Ni-C}}$ (Å)	1.866(2)	1.882(1)	1.911(2)	1.888(2)	1.858(1)	1.805(31)
$d_{\text{M-O}}$ (Å)	—	2.352(1) <sup>a</sup> 2.217(1) <sup>a</sup> 2.459(1) <sup>a</sup>	—	1.897(2) <sup>b</sup>	2.204(1) <sup>c</sup> 2.066(1) <sup>c</sup>	2.030(18) <sup>c</sup>
$d_{\text{C-O}}$ (Å)	1.269(3) 1.313(3)	1.260(1) 1.271(1)	1.247(2) 1.248(2)	1.240(3) 1.296(3)	1.269(2) 1.289(2)	1.298(30) 1.316(30)
$\Delta d_{\text{C-O}}$ (Å)	0.044	0.011	0.001	0.056	0.020	0.018
$\angle \text{O-C-O}$ (°)	119.6(2)	124.0(1)	128.4(2)	123.7(2)	116.5(1)	117.2(26)

<sup>a</sup> M = Na. <sup>b</sup> M = Ni. <sup>c</sup> M = Fe.

CO<sub>2</sub><sup>2-</sup> being shifted to the nickel, the CO<sub>2</sub> moiety is slightly oxidized compared to the sp<sup>2</sup> hybridized carboxylate ligands found in 2 and 4. The larger O–C–O angle (128.4(2)°) of 3 compared to others (124.0(1) and 123.7(2)°) also supports this electronic feature, *vide infra*. Although an η<sup>1</sup>-κC CO<sub>2</sub> coordination mode has been proposed for many CO<sub>2</sub> reduction strategies,<sup>2,3</sup> the only example of a crystallographically identified metal η<sup>1</sup>-κC CO<sub>2</sub> complex is a rhodium CO<sub>2</sub> adduct, Rh(CO<sub>2</sub>)-(Cl)(diars)<sub>2</sub> (diars = *o*-phenylene-bis(dimethylarsine)), reported by the Herskovitz group.<sup>14</sup> According to their C–O bond distances (1.20(2) and 1.25(2) Å) and O–C–O angle (126(2)°), the CO<sub>2</sub> moiety in 3 shares similar structural and electronic features. Thus, compound 3 is a unique example possessing η<sup>1</sup>-κC CO<sub>2</sub> binding, since such a binding mode is unknown for 1<sup>st</sup> row transition metals and is rare in structurally characterized metal–CO<sub>2</sub> adducts.

### Synthesis and characterization of the heterobimetallic nickel–iron CO<sub>2</sub> complex

To gain a better understanding of the role of the second metal ion in the CODH active site, we prepared a heterobimetallic nickel–iron carboxylate species possessing a Ni–CO<sub>2</sub>–Fe

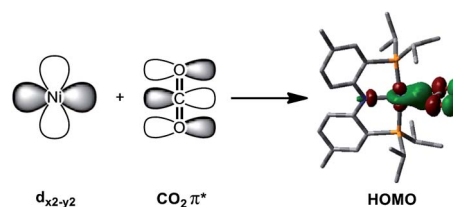


Fig. 2 Combination of the Ni  $d_{x^2-y^2}$  and CO<sub>2</sub>  $\pi^*$  orbitals provides the DFT calculated HOMO of {Na(12-C-4)<sub>2</sub>}{(PNP)Ni-η<sup>1</sup>-CO<sub>2</sub>-κC} (3).

fragment by addition of {(PNP)Fe}<sup>+</sup> to a Ni-η<sup>1</sup>-CO<sub>2</sub>-κC species. To a yellow solution of {Na(12-C-4)<sub>2</sub>}{(PNP)Ni-η<sup>1</sup>-CO<sub>2</sub>-κC} (3) in toluene, a purple solution of (PNP)FeCl was added. The immediate formation of a new orange species (PNP)Ni-μ-CO<sub>2</sub>-κC:κ<sup>2</sup>O,O'-Fe(PNP) (5) was confirmed, using the <sup>1</sup>H NMR spectrum, from the absence of peaks for 3 and (PNP)FeCl and the presence of new paramagnetically shifted signals. The same product was also prepared by substitution of the sodium ion of (PNP)NiCOONa (2) with (PNP)FeCl. The solid-state structure of 5 clearly revealed a dinuclear nickel–iron complex with a bridging CO<sub>2</sub> ligand in the μ<sub>2</sub>-κC:κ<sup>2</sup>O,O' mode (Fig. 3). The Ni and Fe ions are separated by a distance of 4.3690(3) Å. The two C–O bond

Table 2 Selected physical parameters and bond indices from the natural bond orbital analysis

	Ni(PCy <sub>3</sub> ) <sub>2</sub> (η <sup>2</sup> -CO <sub>2</sub> ) <sup>9a</sup>	(dtbpe)Ni(η <sup>2</sup> -CO <sub>2</sub> ) <sup>9d</sup>	(PP <sup>Me</sup> P)Ni(η <sup>2</sup> -CO <sub>2</sub> ) <sup>9f</sup>	3	5
<b>Structural parameters</b>					
$d_{\text{Ni-C}}$ (Å)	1.84(2)	1.868(2)	1.904(1)	1.911(2)	1.858(1)
$d_{\text{Ni-O}}$ (Å)	1.99(2)	1.904(2)	2.191(1)	2.614(1) 2.776(1)	2.718(1) 2.792(1)
$d_{\text{C-O}}$ (Å)	1.17(2) 1.22(2)	1.200(3) 1.266(3)	1.218(2) 1.252(2)	1.248(2) 1.247(2)	1.269(2) 1.289(2)
$\angle \text{O-C-O}$ (°)	133	138.0(2)	135.1(1)	128.4(2)	116.5(1)
$\nu_{\text{CO}_2}$ (cm <sup>-1</sup> )	1740	1724	1682	1620	1510
<b>Wiberg bond indices<sup>a</sup></b>					
Ni–C	—	0.5766	0.5286	0.6143	0.6277
Ni–O	—	0.4300	0.3117	0.1679 0.1358	0.0798 0.0644
C–O	—	1.6927 1.4080	1.6384 1.4701	1.5112 1.4949	1.3993 1.2933

<sup>a</sup> Wiberg bond indices were calculated using single-point calculations, for which geometries were obtained from the XRD data.



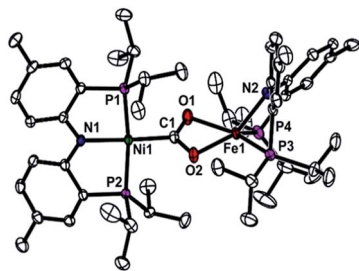


Fig. 3 Displacement ellipsoid (50%) representation for (PNP)Ni- $\mu$ -CO<sub>2</sub>- $\kappa$ C: $\kappa^2$ O, $O'$ -Fe(PNP) (5). Hydrogen atoms are omitted for clarity.

distances are 1.269(2) and 1.289(2) Å, revealing that a significant elongation has occurred due to the iron interaction compared to **3** (Table 1). The bond distances between the iron and both oxygen atoms are 2.204(1) and 2.066(1) Å. The nickel center possesses a square planar geometry ( $\tau_4 = 0.10^{12}$ ). The geometry around the iron is distorted square pyramidal ( $\tau = 0.13$ ,<sup>15</sup> Fig. 3). The O1–C1–O2 angle (116.5°) reflects the sp<sup>2</sup> hybridization of the carboxylate ligand in **5**. In fact, recent crystallographic data of CODH at atomic resolution ( $d_{\min} = 1.03$  Å) revealed that the bound CO<sub>2</sub> molecule ( $\angle$ O–C–O = 117.2(26)°) is a carboxylate anion (CO<sub>2</sub><sup>2-</sup>).<sup>8b,8c</sup> Regarding the similarity between these angles, the carboxylate moiety in **5** might be close to CO<sub>2</sub><sup>2-</sup>. The asymmetric vibration for CO<sub>2</sub> observed at 1510 cm<sup>-1</sup>, which is similar to that observed for the dinickel carboxylate species (**4**) at 1518 cm<sup>-1</sup>, also indicates a reduced state of CO<sub>2</sub>. The effective magnetic moment of **5** was determined using the Evans' method ( $\mu_{\text{eff}} = 4.95 \mu_{\text{B}}$  in C<sub>6</sub>D<sub>6</sub>), which indicated an  $S = 2$  spin state.<sup>16</sup> According to DFT calculations, most of the spin density is located on the iron center (see ESI<sup>†</sup>). For CODH, the unique iron, Fe<sub>u</sub>, was assigned as a high spin iron(II) (ferrous component II, FCII) using Mössbauer spectroscopy,<sup>17</sup> and a low-spin nickel(II) was demonstrated using X-ray absorption spectroscopy (XAS).<sup>18</sup> The current structural and spectroscopic analyses suggest that **5** might share a similar electronic structure to that found in CODH. Gibson classified the  $\mu_2$ - $\kappa$ C: $\kappa^2$ O, $O'$  binding modes of CO<sub>2</sub> into two types according to the difference between the two C–O distances.<sup>19</sup> Due to the two similar C–O distances of the CO<sub>2</sub> moiety, compound **5** ( $\Delta d_{\text{C-O}} = 0.020$  Å) can be assigned as a class I complex.<sup>20</sup> In the dinickel CO<sub>2</sub> species (**4**), the CO<sub>2</sub> molecule is coordinated in a  $\mu_2$ - $\kappa$ C: $\kappa$ O mode with the absence of a Ni2–O2 interaction ( $d_{\text{Ni2-O2}} = 3.14(7)$ ) and two different C–O bond distances ( $\Delta d_{\text{C-O}} = 0.056$  Å). In CODH, CO<sub>2</sub> is coordinated in a  $\mu_2$ - $\kappa$ C: $\kappa$ O fashion between the nickel and iron ions, but the two C–O bond distances are quite comparable ( $\Delta d_{\text{C-O}} = 0.018$  Å), akin to the  $\mu_2$ - $\kappa$ C: $\kappa^2$ O, $O'$  mode. This might be due to hydrogen bonding with the protein matrix, since both the CO<sub>2</sub> oxygens are hydrogen bonded to His93 and Lys563, respectively.<sup>8</sup>

Compound **5** is the first example of a dinuclear nickel–iron–CO<sub>2</sub> complex. While dinuclear CO<sub>2</sub> complexes mostly employ 2<sup>nd</sup> and 3<sup>rd</sup> row transition metals,<sup>19</sup> several bimetallic iron carboxylates (Fe–CO<sub>2</sub>–M, M = Ti, Zr, Sn, Re) have been reported.<sup>5a,5c–e,21</sup> However, such complexes typically possess an Fe–C bond rather than an Fe–O bond with CO<sub>2</sub>. There have been

numerous examples of nickel–iron bimetallic complexes reported for synthetic model studies of NiFe hydrogenase,<sup>22</sup> but a bimetallic complex possessing a Ni- $\mu$ -CO<sub>2</sub>-Fe moiety closely related to CODH chemistry is not known. The Holm group constructed a series of [NiFe<sub>3</sub>S<sub>4</sub>] cubanes as structural model complexes for the [NiFe<sub>4</sub>S<sub>4</sub>] core in CODH.<sup>23</sup> However, the installation of an iron species corresponding to the Fe<sub>u</sub> in CODH and reactions involving CO and CO<sub>2</sub> have not yet been investigated. More recently, the Holm group also reported a bimetallic complex containing nickel and iron supported by a binucleating macrocycle.<sup>24</sup> With respect to CODH chemistry, bridging hydroxo, cyanido and formato species have been generated, however, a Ni- $\mu$ -CO<sub>2</sub>-Fe fragment had not yet been isolated.

### Activation of CO<sub>2</sub> in **3** and **5**

Previously known 4-coordinate Ni–CO<sub>2</sub> complexes possessing an  $\eta^2$ -CO<sub>2</sub> binding mode have a formally zero-valent nickel center, Scheme 1.<sup>9</sup> This suggests limited CO<sub>2</sub> activation in such species. Interestingly, the 5-coordinate nickel CO<sub>2</sub> adduct (PP<sup>Me</sup>P)Ni(CO<sub>2</sub>) also has a similar level of activation of CO<sub>2</sub> based on the C–O bond distances and the O–C–O angle, Table 2. Regarding CO<sub>2</sub> binding and activation, {Na(12-C-4)}{(PNP)Ni- $\eta^1$ -CO<sub>2</sub>- $\kappa$ C} (**3**) is a unique example. It is striking that a neutral pincer-type ligand PP<sup>Me</sup>P (PP<sup>Me</sup>P = PMe[2-P<sup>Pr</sup>Pr<sub>2</sub>-C<sub>6</sub>H<sub>4</sub>]<sub>2</sub>) favors 5-coordinate  $\eta^2$ -CO<sub>2</sub> coordination at a single nickel center, while **3** remains as a 4-coordinate species with  $\eta^1$ -CO<sub>2</sub> coordination.<sup>9f</sup> Although the total number of Ni d-electrons and CO<sub>2</sub>  $\pi^*$ -electrons in both **3** and (PP<sup>Me</sup>P)Ni(CO<sub>2</sub>) is the same, (PP<sup>Me</sup>P)Ni(CO<sub>2</sub>) can be considered as formally Ni(0)–(CO<sub>2</sub>) while **3** can be better described as a Ni(II)–(CO<sub>2</sub><sup>2-</sup>) species. The asymmetric CO<sub>2</sub> stretching frequency for **3** is significantly shifted to a lower vibration, 1620 cm<sup>-1</sup>, compared to those of the Ni- $\eta^2$ -CO<sub>2</sub> complexes (Table 2), which is evidence of a reduced CO<sub>2</sub> moiety in **3**.<sup>9</sup> This may be due to the influence of the *trans* atom: an anionic amide nitrogen *vs.* a neutral phosphorus atom. The anionic nitrogen in **3** electrostatically favors a divalent nickel center, while the neutral  $\pi$ -acidic P atom in the PP<sup>Me</sup>P ligand favors a Ni(0) center. In fact, the PNP ligand typically stabilizes a square planar geometry while the PP<sup>Me</sup>P ligand favors a pseudo-tetrahedral geometry. Thus, **3** prefers to accommodate a divalent nickel center while (PP<sup>Me</sup>P)Ni(CO<sub>2</sub>) prefers Ni(0). However, the reduction state of the CO<sub>2</sub> moiety in **3** is a little ambiguous according to the O–C–O angle. The O–C–O angle in **3** of 128.4(2)° is larger than those of an ideal sp<sup>2</sup> hybridized carbon (120°) and the other nickel(II) carboxylate species **1**, **2** and **4** (119.6(2)°, 124.0(1)° and 123.7(2)°, respectively, Table 1). The O–C–O angle of a CO<sub>2</sub> radical anion (CO<sub>2</sub><sup>•-</sup>) is suggested to be 133°,<sup>25</sup> which is fairly similar to those of the previously reported Ni- $\eta^2$ -CO<sub>2</sub> complexes, Table 2. Thus, the geometry of the CO<sub>2</sub> moiety in **3** may be thought of as being between a CO<sub>2</sub> radical anion and a carboxylate.

Upon addition of iron to compound **3**, the CO<sub>2</sub> is further reduced to carboxylate (CO<sub>2</sub><sup>2-</sup>). The C–O bond distances and O–C–O angle in **5** clearly show a 2-electron reduced state of the CO<sub>2</sub> moiety, Table 2. This was also indicated by the asymmetric CO<sub>2</sub>



vibration observed at  $1510\text{ cm}^{-1}$ , which is significantly lower than those of other  $\text{CO}_2$  species and **3**. The Wiberg bond indices nicely agree with the bond distances, Table 2. These analyses of a series of nickel- $\text{CO}_2$  compounds demonstrate how the degree of  $\text{CO}_2$  activation can be tuned by incorporating a distinct electronic coordination environment at the metal center, and may have parallels to the efficient  $\text{CO}_2$  conversion found in CODH.

In order to study further activation of the bound  $\text{CO}_2$  via C–O bond cleavage, protonation of **3** and **5** was attempted. Our group previously reported that reversible C–O bond cleavage/formation occurs with a nickel hydroxycarbonyl species (**1**).<sup>10</sup> From reaction of **3** with 1 equiv. of  $\text{HBF}_4 \cdot \text{Et}_2\text{O}$ , a nickel hydroxycarbonyl species (**1**) was produced and isolated with a 74% yield. A similar reaction of **3** with 2 equiv. of  $\text{HBF}_4 \cdot \text{Et}_2\text{O}$  resulted in the formation of a carbonyl species  $\{(\text{PNP})\text{NiCO}\}\{\text{BF}_4\}$  in 75% yield, revealing that two sequential protonations can occur with compound **3** possessing a  $\text{Ni}-\eta^1\text{-CO}_2\text{-}\kappa\text{C}$  moiety, which are key steps in the transformation of  $\text{CO}_2$  to CO. Although protonation of compound **5** seems to produce **1** and  $\{(\text{PNP})\text{NiCO}\}\{\text{BF}_4\}$ , unfortunately, their yields were not clear due to thermal decomposition of **5** and the generation of multiple products. Demetallation of the iron seems to be one of the decomposition processes.

## Conclusions

In conclusion, the generation of unprecedented nickel-carbon dioxide adducts possessing a Ni–C bond accommodated by a (PNP)Ni scaffold was accomplished. A mononuclear  $\text{CO}_2$  adduct  $\{\text{Na}(12\text{-C-4})_2\}\{(\text{PNP})\text{Ni}-\eta^1\text{-CO}_2\text{-}\kappa\text{C}\}$  (**3**) and a dinuclear nickel-iron carboxylate species  $(\text{PNP})\text{Ni}-\mu\text{-CO}_2\text{-}\kappa\text{C}:\kappa^2\text{O},\text{O}'\text{-Fe}(\text{PNP})$  (**5**) were synthesized successfully. While the solid state structure of **3** revealed a rare  $\eta^1\text{-}\kappa\text{C}$  binding mode, compound **5** was structurally characterized to reveal a unique class I type  $\mu_2\text{-}\kappa\text{C}:\kappa^2\text{O},\text{O}'$  binding mode. This heterobimetallic  $\text{CO}_2$  adduct is the first example of a nickel-iron carboxylate species, of which the structural and electronic features are reminiscent of those of the  $\text{Ni}-\mu\text{-CO}_2\text{-Fe}$  fragment found in the C-cluster of CODH. Comparison of the  $\eta^1\text{-CO}_2\text{-}\kappa\text{C}$  species **3** and dinuclear  $\text{Ni}-\mu\text{-CO}_2\text{-Fe}$  species **5** with previously reported  $\text{Ni}-\text{CO}_2$  adducts suggested that the  $\text{CO}_2$  ligand can be stabilized and activated by interaction with the second metal. Protonation of **3** produces a nickel carbonyl species  $\{(\text{PNP})\text{NiCO}\}\{\text{BF}_4\}$  via C–O bond cleavage, while the reactivity of **5** is limited. Further studies on incorporating a stable iron species and the subsequent reactivity toward protonation are currently underway.

## Acknowledgements

This work was supported by the C1 Gas Refinery Program (NRF-2015M3D3A1A01064880) through the National Research Foundation of Korea (NRF-2015R1A2A2A01004197), and KAIST and the Aramco Overseas Company. This work was also supported by the Supercomputer Center/Korea Institute of Science and Technology (KSC-2015-S1-0005).

## Notes and references

- (a) Q. Liu, L. Wu, R. Jackstell and M. Beller, *Nat. Commun.*, 2015, **6**, 5933; (b) M. Aresta, A. Dibenedetto and A. Angelini, *Chem. Rev.*, 2014, **114**, 1709; (c) M. Aresta, *Carbon Dioxide as Chemical Feedstock*, Wiley-VCH, Weinheim, 2010.
- (a) J. Qiao, Y. Liu, F. Hong and J. Zhang, *Chem. Soc. Rev.*, 2014, **43**, 631; (b) C. Finn, S. Schnittger, L. J. Yellowlees and J. B. Love, *Chem. Commun.*, 2012, **48**, 1392; (c) E. Fujita, *Coord. Chem. Rev.*, 1999, **185–186**, 373.
- (a) J. Song, E. L. Klein, F. Neese and S. Ye, *Inorg. Chem.*, 2014, **53**, 7500; (b) M. R. Dubois and D. L. Dubois, *Acc. Chem. Res.*, 2009, **42**, 1974; (c) E. E. Benson, C. P. Kubiak, A. J. Sathrum and J. M. Smieja, *Chem. Soc. Rev.*, 2009, **38**, 89.
- (a) M. Devillard, R. Declercq, E. Nicolas, A. W. Ehlers, J. Backs, N. Saffon-Merceron, G. Bouhadir, J. C. Sloopweg, W. Uhl and D. Bourissou, *J. Am. Chem. Soc.*, 2016, **138**, 4917; (b) S. J. K. Forrest, J. Clifton, N. Fey, P. G. Pringle, H. A. Sparkes and D. F. Wass, *Angew. Chem., Int. Ed.*, 2015, **54**, 2223.
- (a) M. Hirano, M. Akita, K. Tani, K. Kumagai, N. C. Kasuga, A. Fukuoka and S. Komiyama, *Organometallics*, 1997, **16**, 4206; (b) K. E. Litz, K. Henderson, R. W. Gourley and M. M. B. Holl, *Organometallics*, 1995, **14**, 5008; (c) J. R. Pinkes, B. D. Steffey, J. C. Vites and A. R. Cutler, *Organometallics*, 1994, **13**, 21; (d) J. R. Pinkes and A. R. Cutler, *Inorg. Chem.*, 1994, **33**, 759; (e) J. C. Vites, B. D. Steffey, M. E. Giuseppetti-Dery and A. R. Cutler, *Organometallics*, 1991, **10**, 2827; (f) E. G. Lundquist, J. C. Huffman, K. Folting, B. E. Mann and K. G. Caulton, *Inorg. Chem.*, 1990, **29**, 128; (g) E. G. Lundquist, J. C. Huffman and K. G. Caulton, *J. Am. Chem. Soc.*, 1986, **108**, 8309; (h) S. Gambarotta, F. Arena, C. Floriani and P. F. Zanazzi, *J. Am. Chem. Soc.*, 1982, **104**, 5082; (i) G. Fachinetti, C. Floriani and P. F. Zanazzi, *J. Am. Chem. Soc.*, 1978, **100**, 7405.
- (a) C. W. Machan and C. P. Kubiak, *Dalton Trans.*, 2016, DOI: 10.1039/C6DT01956K, in press; (b) S. Bagherzadeh and N. P. Mankad, *J. Am. Chem. Soc.*, 2015, **137**, 10898; (c) O. Cooper, C. Camp, J. Pécaut, C. E. Kefalidis, L. Maron, S. Gambarelli and M. Mazzanti, *J. Am. Chem. Soc.*, 2014, **136**, 6716; (d) J. P. Krogman, B. M. Foxman and C. M. Thomas, *J. Am. Chem. Soc.*, 2011, **133**, 14582; (e) B. D. Steffey, C. J. Curtis and D. L. DuBois, *Organometallics*, 1995, **14**, 4937.
- M. Can, F. A. Armstrong and S. W. Ragsdale, *Chem. Rev.*, 2014, **114**, 4149.
- (a) J.-H. Jeoung and H. Dobbek, *Science*, 2007, **318**, 1461; (b) J. Fessler, J.-H. Jeoung and H. Dobbek, *Angew. Chem., Int. Ed.*, 2015, **54**, 8560; (c) M. W. Ribbe, *Angew. Chem., Int. Ed.*, 2015, **54**, 8337.
- (a) M. Aresta, C. F. Nobile, V. G. Albano, E. Forni and M. Manassero, *J. Chem. Soc., Chem. Commun.*, 1975, 636; (b) M. Aresta and C. F. Nobile, *J. Chem. Soc., Dalton Trans.*, 1977, 708; (c) A. Döhring, P. W. Jolly, C. Krüger and



- M. J. Romão, *Z. Naturforsch., B: J. Chem. Sci.*, 1985, **40**, 484; (d) J. S. Anderson, V. M. Iluc and G. L. Hillhouse, *Inorg. Chem.*, 2010, **49**, 10203; (e) R. Beck, M. Shoshani, J. Krasinkiewicz, J. A. Hatnean and S. A. Johnson, *Dalton Trans.*, 2013, **42**, 1461; (f) Y.-E. Kim, J. Kim and Y. Lee, *Chem. Commun.*, 2014, **50**, 11458.
- 10 C. Yoo, J. Kim and Y. Lee, *Organometallics*, 2013, **32**, 7195.
- 11 C. Yoo and Y. Lee, *Inorg. Chem. Front.*, 2016, **3**, 849.
- 12 L. Yang, D. R. Powell and R. P. Houser, *Dalton Trans.*, 2007, 955.
- 13 C. Yoo, S. Oh, J. Kim and Y. Lee, *Chem. Sci.*, 2014, **5**, 3853.
- 14 J. C. Calabrese, T. Herskovitz and J. B. Kinney, *J. Am. Chem. Soc.*, 1983, **105**, 5914.
- 15 A. W. Addison, T. N. Rao, J. Reedijk, J. van Rijn and G. C. Verschoor, *J. Chem. Soc., Dalton Trans.*, 1984, 1349.
- 16 (a) D. F. Evans, *J. Chem. Soc.*, 1959, 2003; (b) S. K. Sur, *J. Magn. Reson.*, 1989, **82**, 169.
- 17 Z. Hu, N. J. Spangler, M. E. Anderson, J. Xia, P. W. Ludden, P. A. Lindahl and E. Münck, *J. Am. Chem. Soc.*, 1996, **118**, 830.
- 18 W. Gu, J. Seravalli, S. W. Ragsdale and S. P. Cramer, *Biochemistry*, 2004, **43**, 9029.
- 19 D. H. Gibson, *Chem. Rev.*, 1996, **96**, 2063.
- 20 Classification of the  $\mu_2\text{-}\kappa\text{C}:\kappa^2\text{O},\text{O}'$  binding modes of  $\text{CO}_2$  for a bimetallic center (M and M'): while the  $\text{CO}_2$  coordinates *via* a M–C bond, class I complexes have the two oxygen atoms of the  $\text{CO}_2$  ligand symmetrically bonded to M' and class II complexes possess two asymmetric M'–O bonds.
- 21 (a) D. H. Gibson, J. F. Richardson and T.-S. Ong, *Acta Crystallogr., Sect. C: Cryst. Struct. Commun.*, 1991, **47**, 259; (b) D. H. Gibson, M. Ye and J. F. Richardson, *J. Am. Chem. Soc.*, 1992, **114**, 9716; (c) D. H. Gibson, J. F. Richardson and O. P. Mbadike, *Acta Crystallogr., Sect. B: Struct. Sci.*, 1993, **49**, 784; (d) D. H. Gibson, M. Ye, J. F. Richardson and M. S. Mashuta, *Organometallics*, 1994, **13**, 4559; (e) D. H. Gibson, M. Ye, B. A. Sleadd, J. M. Mehta, O. P. Mbadike, J. F. Richardson and M. S. Mashuta, *Organometallics*, 1995, **14**, 1242; (f) M. Lutz, M. Haukka, T. A. Pakkanen and L. H. Gade, *Organometallics*, 2001, **20**, 2631.
- 22 (a) S. Kaur-Ghumaan and M. Stein, *Dalton Trans.*, 2014, **43**, 9392; (b) A. C. Marr, D. J. E. Spencer and M. Schröder, *Coord. Chem. Rev.*, 2001, **219–221**, 1055.
- 23 (a) S. Ciurli, P. K. Ross, M. J. Scott, S.-B. Yu and R. H. Holm, *J. Am. Chem. Soc.*, 1992, **114**, 5415; (b) R. Panda, C. P. Berlinguette, Y. Zhang and R. H. Holm, *J. Am. Chem. Soc.*, 2005, **127**, 11092; (c) J. Sun, C. Tessier and R. H. Holm, *Inorg. Chem.*, 2007, **46**, 2691.
- 24 D. Huang and R. H. Holm, *J. Am. Chem. Soc.*, 2010, **132**, 4693.
- 25 (a) D. W. Ovenall and D. H. Whiffen, *Mol. Phys.*, 1961, **4**, 135; (b) J. W. Rabalais, J. M. McDonald, V. Scherr and S. P. McGlynn, *Chem. Rev.*, 1971, **71**, 73.

